JOURNAL OF AGRICULTURAL AND FOOD CHEMISTRY

J. Agric. Food Chem. **2008,** *56,* 433–441 **433**

Profiling the *Monascus pilosus* Proteome during Nitrogen Limitation

WUN-YUAN LIN,[†] JUI-YUN CHANG,[†] CHIH-HSUAN HISH,[†] AND TZU-MING PAN*[,‡]

Department of Food Science, Nutrition, and Nutraceutical Biotechnology, Shih Chien University, Taipei, Taiwan, and Institute of Microbiology and Biochemistry, National Taiwan University, Taipei, Taiwan, Republic of China

Monascus species have the unique ability to economically produce many secondary metabolites. However, the influence of nitrogen limitation on *Monascus* secondary metabolite production and metabolic performance remains unclear. Varying the carbon/nitrogen (C/N) ratios in the range from 20 to 60 in cultivation of *Monascus pilosus* by glucose nitrate medium, our resulting data showed that red pigment production was significantly suppressed and more sensitive to nitrogen limitation than cellular biomass growth at a C/N ratio of 60. Using a comparative proteomic approach, combining two-dimensional gel electrophoresis, matrix-assisted laser desorption ionization time-of-flight/time-of-flight liquid chromatography–mass spectrometry, and tandem mass spectrometry, proteins with modified expression in the nitrogen-limited (C/N ratio 60) *Monascus* filamentous cells were identified. The results revealed that the deregulated proteins identified were involved in amino acid biosynthesis, protein translation, antioxidant-related enzymes, glycolysis, and transcriptional regulation. The results suggested that, under nitrogen limitation-induced suppression of protein translation and of expression of the related energy-generating enzymes, nitrogen limitation induced a switch of metabolic flux from glycolysis to the tricarboxylic acid (TCA) cycle for maintaining cellular energy homeostasis, resulting in repression of the metabolic shift of the polyketide biosynthesis pathway for red pigment production.

KEYWORDS: ***Monascus*; pigments; polyketides; nitrogen limitation; proteomics**

INTRODUCTION

Monascus has been extensively used in fermented food and folk medicine for thousands of years in China. *Monascus* produces many types of polyketide secondary metabolites, which have enormous commercial value and many functional properties, including a group of yellow pigments, ankaflavin and monascin, orange pigments, monascorubrin and rubropunctatin, red pigments, monascorubramine and rubropunctamine (*1*), monacolin K (also known as lovastatin), and the antibacterial compound citrinin (*2, 3*). Secondary polyketide biosynthesis involves using acetyl-CoA as the building block, and subsequent steps of transformation, including reduction and oxidative rearrangement, yield several precursor intermediates to form polyketides (*4*).

In industrial fermentation, microbial cultivation is always in some way controlled by limitation of the availability of nutrients. Carbon sources usually fulfill their energetic role through catabolism while priming anabolism with carbon intermediates for biomass synthesis. On the contrary, nitrogen sources act principally as anabolic substrates. Nitrogen is a major component of nearly all of the complex macromolecules central to cellular structure and function of all living organisms (*5*). Accordingly, nitrogen content in medium greatly influences the synthesis of fungal biomass and the accumulation of secondary metabolites. Elaborate control mechanisms governing nitrogen metabolism have been discovered in *Saccharomyces cerevisiae* and *Aspergillus nidulans* (*5, 6*). However, in *Monascus*, little is known concerning nitrogen metabolism and its regulation in metabolic performance for polyketide secondary metabolite production.

Proteome analysis utilizes two-dimensional gel electrophoresis (2-DE) to separate complex protein mixtures, which is followed by in-gel tryptic digestion and mass spectrometry for protein identification. The proteome provides a better understanding of the dynamic and overall view of the cell machinery under various conditions. In previous studies, we found that, in *Monascus* cultivation, the secondary metabolites, pigments, γ-aminobutyric acid (GABA), and monacolin K, accumulated during the stationary phase of culture (*7*). However, fungal cells in the stationary phase are generally more tolerant to stress conditions than are cells in the other growth phases (*8*). The aim of this work was to characterize the nitrogen limitation-induced protein profiles in the cultured *Monascus* filamentous cells using proteome analysis and to extend our understanding of nitrogen metabolism and its regulation in metabolic performance concerning cellular biomass growth and red pigment

* Author to whom correspondence should be addressed (telephone, +886-2-3366-4519; fax, +886-2-2362-7044; e-mail, tmpan@ntu.edu.tw).

[†] Shih Chien University.

[‡] National Taiwan University.

10.1021/jf072420e CCC: $40.75
Published on Web 12/21/2007

production. Because, in the previous study, red pigments are the major produced pigments in cultivation of *Monascus pilosus* BCRC 31527 (*9*), the polyketide secondary metabolite investigated was focused on red pigments. Varying the carbon/nitrogen (C/N) ratios in the range from 20 to 60 with no severe nitrogen limitation in *Monascus* cultivation, our resulting data revealed that the red pigment production was more sensitive than cellular biomass growth under C/N ratio 60 nitrogen limitation. Our results suggested that, under nitrogen limitation-induced suppression of protein translation and of expression of the related energy-generating enzymes, nitrogen limitation induced a switch of metabolic flux from glycolysis to the tricarboxylic acid (TCA) cycle for maintaining cellular energy homeostasis, resulting in repression of the metabolic shift of the polyketide biosynthesis pathway for red pigment production.

MATERIALS AND METHODS

Strain and Culture Conditions. The *M. pilosus* BCRC 31527 strain was subjected to proteome analysis. This strain was obtained from the Bioresource Collection and Research Center (BCRC) in Taiwan and is a high pigment-producing strain in a previous study (*9*). This strain was maintained and sporulated on potato dextrose agar (Merck, Darmstadat, Germany) in stock culture. The defined medium for growth of the control group (C/N ratio 20) was glucose nitrate medium containing 3% (w/v) glucose, 0.15% (w/v) $NaNO_3$, 0.1% (w/v) $MgSO_4 \cdot 7H_2O$, and 0.25% (w/v) KH_2PO_4 following the method of previous studies (*10*). For the nitrogen-limited cultivation treatments with C/N ratios of 30, 40, and 60, the $NaNO_3$ ingredient used in the medium was modified to 0.1%, 0.075%, and 0.05% (w/v), respectively, while the levels of the other ingredients were kept constant. The spores were prepared by growth on potato dextrose agar slants for 15 days at 32 °C and were washed with a sterile phosphate buffer (50 mM, pH 7.0). In submerged cultivation, a suspension of 10^8 spores was used to inoculate a 1 L baffled Erlenmeyer flask containing 250 mL of the control and nitrogen-limited media (the pH of the medium was adjusted to 6.2 with 1 N HCl or 1 N NaOH before sterilization), which were then cultivated at 32 °C for 10 days on a rotary shaker at 150 rpm in triplicate.

Reagents and Materials. The 2-DE reagents, including acrylamide solution (25%), dithiothreitol (DTT), sodium dodecyl sulfate (SDS), trifluoroacetic acid (TFA), urea, iodoacetamide (IAA), thiourea, 3-[(3-cholamidopropyl)dimethylammonio]-1-propanesulfonate (CHAPS), Immobiline dry strips, immobilized pH gradient (IPG) buffer, IPG cover mineral oil, Tris base, and the protein assay kit, were purchased from Bio-Rad (Hercules, CA). Sulfanilamide, *N*-(1-naphthyl)ethylenediamine dihydrochloride, phenylmethanesulfonyl fluoride (PMSF), sorbitol, and α-cyano-4-hydroxycinnamic acid (CHCA) were purchased from Sigma (St. Louis, MO). Sypro Ruby stain was purchased from Amersham Biosciences (Piscataway, NJ). Trypsin (modified) was obtained from Promega (Madison, WI). ZipTip C_{18} microcolumns were purchased from Millipore (Bedford, MA). Other reagents used in this work were of analytical grade and purchased from local suppliers.

Pigment Extraction and Measurement. Estimation of red pigment production was performed as previously described (*11, 12*). After fermentation, the cultured mycelia from a single flask (containing 250 mL of growth substrate) were filtered, washed with distilled water, and extracted with 80 mL of 95% ethanol for 12 h. The filtered solution and extract were made into aliquots, and the absorbance at 500 nm was measured in a spectrophotometer (Thermo Helios α, Waltham, MA). The absorbance in the filtered solution and extract was added to give the total absorbance of red pigments produced. For dry cell growth mass, the mycelia from a single flask (250 mL of growth substrate) after extraction were lyophilized in a vacuum freeze dryer (EYELA FDU-540, Tokyo, Japan) for 2 days.

Protein Preparation for 2-DE. For 2-DE analysis, the cultured filamentous cells were collected during the early stationary phase at the fifth day of cultivation. Preparation of 2-DE protein extracts was performed as described in the previous study (*9*). Briefly, after sonication and disruption with a continuous type presser (Constant Systems Ltd., Northants, England), proteins were extracted in a Tris-HCl buffer. After centrifugation at 40000*g* and 4 °C, the resulting supernatant was mixed with ice-cold trichloroacetic acid and DTT, incubated at −20 °C overnight, and washed with ice-cold acetone [containing 0.1% (w/v) DTT] to obtain the cellular protein pellets.

IEF and 2-DE Separation. Isoelectric focusing (IEF) was conducted using Amersham Biosciences IPGphor. IPG strips (13 cm; Amersham Biosciences), with a nonlinear pH range from 3 to 10, were used for protein separation by following the protocol described previously (*10*). The protein pellet was solubilized completely in sample buffer [7 M urea, 2 M thiourea, 4% (w/v) CHAPS, 2% ampholine, 65 mM DTT, with a trace of bromophenol blue]. After 10 min of centrifugation at 18000*g* and 4 °C, the supernatant containing 300 μg of cellular protein was loaded onto the dried IPG strip. Protein content was determined by the Bradford method (protein assay kit; Bio-Rad). The dried IPG strips were actively rehydrated with the loading of protein samples (300 μg/350 μL) at 10 V for 10 h at 20 °C in the ceramic strip holder. Focusing was performed in six steps (100 V for 1 h, 250 V for 1 h, 500 V for 1 h, 1000 V for 1 h, 4000 V for 1 h, and 8000 V for 50000 V/h, total of 55970 V/h) at 20 °C. The focused IPG strips were equilibrated with equilibration buffer [50 mM Tris-HCl, pH 8.8, 6 M urea, 30% (v/v) glycerol, 2% (w/v) SDS, and 2% (w/v) DTT] three times for 10 min each and then resolved in a 10% polyacrylamide gel 1.5 mm thick on a vertical SDS−PAGE system (13.5 cm × 13.5 cm, Protean II xi cell; Bio-Rad) at a constant voltage of 10 mA for 0.5 h and 30 mA for 4 h. 2-DE was run in pairs side by side and performed in triplicate for each pair of samples to ensure reproducibility.

Image Acquisition and In-Gel Digestion. Gel image analysis was performed using a Typhoon 9200 scanner (Amersham Biosciences). The Sypro Ruby-stained gels were digitized with the PDQuest software (Bio-Rad). Protein spots were quantified and characterized with respect to their molecular mass (M_r) and isoelectric point (p*I*) by bilinear interpolation between landmark features on each image previously calibrated with respect to internal 2-DE standards (Bio-Rad). 2-DE gel data were normalized by dividing each spot quantity by the total quantity of all of the valid spots in the 2-DE gel image. For each matched spot, the mean of the three quantity values from triplicate 2-DE gels was calculated. The differences in protein expression between the control and the treated group were analyzed by Student's *t*-test, and *P* values <0.05 were considered statistically significant. The Sypro Ruby-stained protein spots were manually excised for in-gel digestion with trypsin as described in the previous study (*10*). Briefly, proteins selected for analysis were in-gel reduced, alkylated, and digested with 12.5 ng/mL sequencing-grade trypsin in 25 mM NH_4HCO_3 (pH 8.5).

Protein Identification and Data Analysis. A MALDI-TOF/TOF mass spectrometer (4700 proteomics analyzer; Applied Biosystems, Framingham, MA) equipped with a Nd:YAG laser (355 nm wavelength, <500 ps pulse, and 200 Hz repetition rate in both MS and MS/MS modes) was employed to obtain peptide mass spectra. Peptide mass spectra were recorded, and parameters for spectra acquisition were used as stated previously (*9*). Briefly, the tryptic-digested peptide samples were premixed with a matrix solution of 5 mg/mL CHCA and dissolved in 50% acetonitrile (ACN) with 0.1% formic acid. MALDI-TOF/TOF-MS detection and MS/MS sequencing of isopeptides were operated in the reflector mode. Proteins were identified by peptide fingerprinting to search against protein sequences from the SwissPort, NCBI, and/or MSDB databases using MASCOT (http://www.matrixscience.com). The criteria for database matching were ±25 ppm mass tolerance and corresponding M_r and p*I* values. The species of origin was restricted to fungi and bacteria taxonomy categories.

RESULTS

Biomass Growth and Red Pigment Production of *M. pilosus* BCRC 31527 under Nitrogen Limitation. To investigate how the polyketide pigment production and metabolism of *M. pilosus* BCRC 31527 were affected by nitrogen limitation, we performed *M. pilosus* BCRC 31527 cultivations with C/N ratios varying at 20, 30, 40, and 60 with C/N ratios ≤60. Because of preliminary experiments with C/N ratios >60 in the feed media, the *Monasus* culture biomass growth apparently

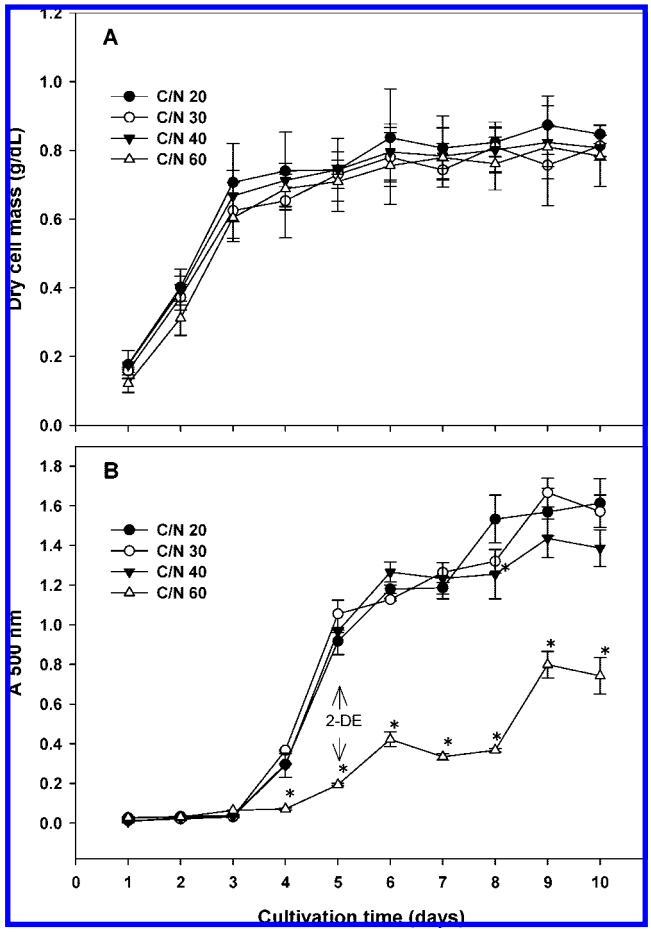

Figure 1. Effect of nitrogen-limited cultivation with C/N ratios 20, 30, 40, and 60 in glucose nitrate media (see Materials and Methods) on the dry cell mass (part **A**) and red pigment production (absorbance, *A* 500 nm; part **B**) of *M. pilosus* BCRC 31527 during culture development in batch-type submerged fermentation on a rotary shaker at 32 °C and 150 rpm for 10 days. The data shown were the means ± SEM from three independent experiments. An asterisk indicates the values at each cultivated day that were significantly different from the C/N ratio 20 control group (Student's *t*-test; $P < 0.05$). 2-DE: the day the cells were harvested and proteins extracted for 2-DE gel analysis.

was inhibited during 10 days of submerged cultivation; simultaneously, red pigment production was completely blocked (data not shown). Regarding the substrate medium used, a defined medium, glucose nitrate medium, was used for easy control of C/N ratios instead of a complex rice substrate. It also is a better growth substrate for induction of high pigment productivity in *Monascus* in previous studies (*10, 11*).

In our resulting data, the cultured filamentous cellular biomass growths among the range of C/N ratios from 20 to 60 revealed no significant difference ($P > 0.05$) for each cultivated day during 10 days of cultivation (**Figure 1A**). Together in a similar growth tendency, after 3 days of log phase growth, their maximum dry cell mass reached 0.87, 0.81, 0.82, and 0.81 g/dL, corresponding to C/N ratios from 20 to 60 treatments at stationary phase. Furthermore, the red pigment production in the C/N ratio 20−40 groups was observed with no statistically significant difference during cultivation (**Figure 1B**). Interestingly, compared to the C/N ratio 20 control group, the red pigment production of the C/N ratio 60 group was significantly suppressed ($P < 0.05$) after the fourth day of cultivation. In other words, in this work, for *M. pilosus* BCRC 31527 under the nitrogen-limited treatment, the culture of the C/N ratio 60 group displayed sensitivity to nitrogen limitation for red pigment formation; on the contrary, its cellular biomass growth was not significantly affected under this nitrogen limitation condition.

Protein Identification. In the previous studies, most of the secondary metabolites in the *Monascus* culture accumulated during the stationary phase of cultivation (*7*). To characterize differences in nitrogen metabolism and its regulation between the primary cellular biomass growth and secondary metabolite pigment formation in *M. pilosus* BCRC 31527 cells in response to nitrogen limitation at the stationary phase, proteins extracted from the cultured filamentous cells of the control and the C/N ratio 60 group at the fifth day during the early stationary phase were subjected to proteome analysis (**Figure 1**). Compared to bacterium, plant, and animal proteomics, proteomics in filamentous fungi are still at an early stage of development (*13*). Although 2-DE is a powerful tool for the separation and quantification of proteins, it has limitations in resolving proteins with high M_r or p*I* values. In preliminary analysis of this work, a comparison between using a 10–18% nonlinear gradient and a constant 10% SDS−PAGE for separation of proteins in the second dimension (*9*) showed that the constant 10% SDS−PAGE was better in reproducibility and resolution of high M_r proteins. Additionally, because of comparison to 2-DE gels of human cells as described previously (*14*), the number of protein spots of *Monascus* 2-DE gels was less. To avoid quantitative loss of high p*I* proteins, instead of the pH range from 4 to 7, IPG strips in the pH range from 3 to 10 were applied in this approach.

After analysis of the resulting images, a total of 65 protein spots from the cellular protein preparation gels were cut and first identified by MALDI-TOF/TOF-MS. Identified proteins are highlighted and numbered on the 2-DE gel pictures shown in **Figure 2**, and detailed information concerning these proteins can be found in **Table 1**. Three proteins, for which a positive identification could not be made using PMF alone, were further confirmed by MS/MS and LC-MS. Of the 65 protein spots excised for MALDI-TOF/TOF analysis, 22 proteins were identified, giving a 34% identification rate. In this work, using cross-species identification (CSI) to search the PMF data (*15*), the identified proteins were matched to known proteins from the fungus species to other microorganisms. The categories of identified proteins included hydroylases, isomerases, lyases, transcriptional regulators, and oxidoreductases.

Proteome Response to Nitrogen-Limited Cultivation. To extend the understanding of nitrogen metabolism and its regulation in the cultured *Monascus* cells in response to nitrogen limitation, a comparison of the deregulated proteins identified between the control and the nitrogen-limited media of C/N ratio 60 was performed using PDQuest program-aided (Bio-Rad) analysis (**Table 1**). In this work, a total of 22 proteins were identified. Of the 22 protein spots identified, 17 were downregulated and only 5 were upregulated in the nitrogen-limited sample (**Table 1**). The downregulated proteins identified included highly conserved aminoacyl-tRNA synthetases, glutaminyl-tRNA synthase (GluRS), cysteinyl-tRNA synthetase (CysRS), arginyl-tRNA synthetase (ArgRS), and valyl-tRNA synthetase (ValRS) (*16*), several amino acid synthesis-related enzymes, antioxidant-related enzymes, glutamate−cysteine ligase (GCL), superoxide dismutase (SOD), and peroxidase (Px), and two energy-related enzymes, ATP synthase F1 γ subunit (ATPase γ) and adenylate kinase (AK). In comparison, interestingly, only 5 identified proteins, including three glycolysis-related enzymes, enolase (EN), phosphoenolpyruvate carboxylase (PEPC), and UDP-glucose 4-epimerase (GlcE), and two transcriptional regulation enzymes, DNA-directed RNA polymerase β chain

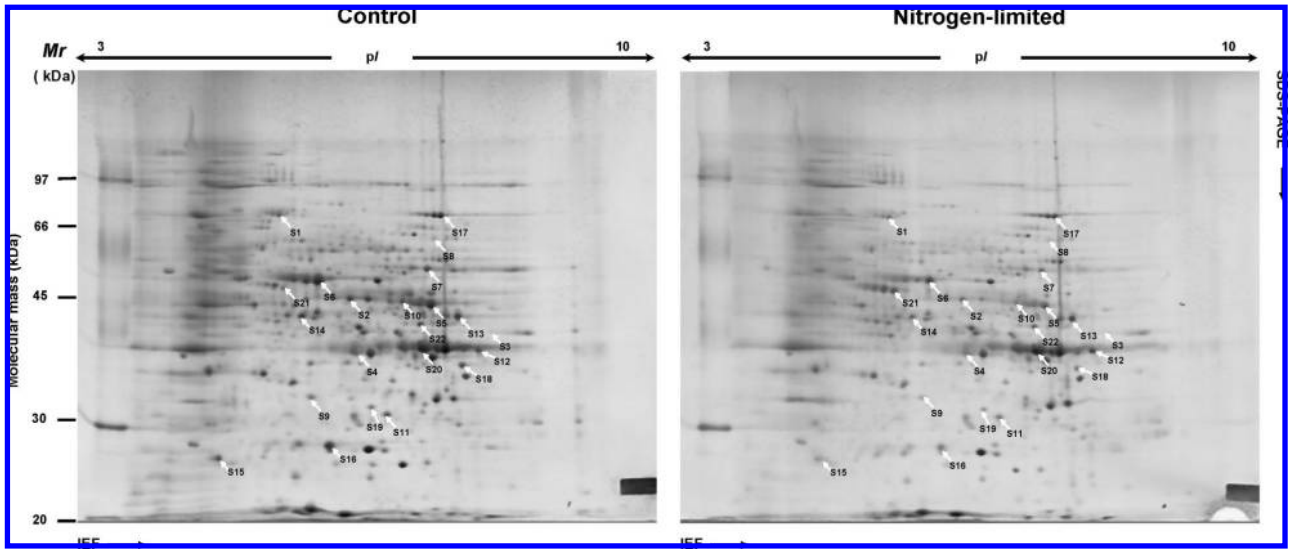

Figure 2. Comparative 2-DE gel analyses of cellular proteins of *M. pilosus* BCRC 31527 cultivated in the C/N ratio 20 control medium and the C/N ratio 60 nitrogen-limited medium with submerged fermentation at 32 °C and 150 rpm at the fifth day of cultivation. The cellular protein (300 μg/350 μL) extracts were displayed across a 13 cm IPG strip (pH 3–10) in the first dimension and 10% SDS−PAGE in the second dimension and stained with Sypro Ruby. Isoelectric points (p*I*) and molecular masses (M_r) are marked on the horizontal and vertical axes, respectively. Protein spots marked on the maps with arrows and numbers represent the 22 identified proteins analyzed with the PDQuest program. Details of the proteins are given in **Table 1**.

(RNAPβ) and histone deacetylase 1 (HDA), revealed upregulation in the nitrogen-limited sample.

DISCUSSION

Nitrogen metabolism in fungi is a tightly regulated process that confers fungi the ability to use limited nitrogen sources for cell survival. Efficient regulation of this process likely allows fungi to exploit various ecological niches (*17*). In this work, the resulting data revealed that, in *M. pilosus* BCRC 31527, the metabolic performance in red pigment production showed significant suppression and was more sensitive to nitrogen limitation than cellular biomass growth under the C/N ratio 60 nitrogen-limited condition. On the contrary, the changes in the cellular biomass growth under the C/N ratios from 20 to 60 were not significantly different (**Figure 1**).

In our proteomic analysis, seven amino acid synthesis-related enzymes, including CSase, MAT, MTase, OTC, ACCD, trpA, and dadA, were cooperatively downregulated in the nitrogen-limited sample (**Table 1**). CSase, the enzyme responsible for the condensation of *O*-acetylserine with sulfide, is the major enzyme for the synthesis of cysteine, which, in turn, serves as an intermediate in the synthesis of methionine and *S*-adenosylmethionine (AdoMet) (*18*). Sulfur amino acids, especially cysteine and methionine, are essential for the growth and activities of all cells (*18*). Following the CSase downregulation, simultaneously MAT and MTase, both in the subsequent downstream pathway of CSase, were also downregulated. MAT is the enzyme that catalyzes the formation of AdoMet from methionine and ATP (*19*). Interestingly, MTase, which catalyzes the methyl transfer from the ubiquitous AdoMet to either nitrogen, oxygen, or carbon atoms in metabolism, is involved in amino acid synthesis (such as lysine and threonine) and posttranslational protein modification (*20*). In *S. cerevisiae*, it is known that AdoMet acts as the metabolite responsible for sulfur metabolite repression in allosteric control of assimilatory pathways (*18*). In the filamentous fungi *Neurospora*, methionine and AdoMet metabolism are governed by complex regulatory circuits, which control the expression of the catabolic enzymes that are involved in amino acid biosynthesis (*21*). The observed downregulation of CSase, MAT, and MTase together may be a reflection of repression in sulfur metabolite amino acid synthesis in the nitrogen-limited cultured filamentous cells. Moreover, ACCD, a pyridoxal phosphate-dependent enzyme, degrades aminocyclopropane-1-carboxylate (ACC) into α-ketoglutarate (the precursor of the amino acids valine and threonine) (*22*). Interestingly, in bacteria, yeast, and fungi, ACC is formed from AdoMet via a ring closing γ-displacement reaction (*22*). Here, the coordinated downregulated expression of CSase, MAT, and MTase coupled with the decreased ACCD expression together in sequential metabolism steps may lead to a decrease in valine and threonine pools, which, in turn, affects valine- and threonine-related protein biosynthesis in translation. In addition, two other amino acid synthesis-related enzymes, OTC, involved in the arginine biosynthetic pathway (*23*), and trpA, an enzyme in the last two reactions of tryptophan biosynthesis (*24*), were also downregulated in the nitrogen-limited sample. In *S. cerevisiae*, nitrogen limitation in cultivation has great influence on the synthesis of the intracellular amino acid pools (*8*). Accordingly, in this work, the resulting codownregulated expression of these amino acid synthesis-related enzymes in the nitrogen-limited cultured *Monascus* cells at C/N ratio 60 suggested a decrease in the intracellular amino acid pools in response to a lack of available nitrogen source under nitrogen limitation in the intrinsic properties of the *Monascus* nitrogen metabolism.

Protein biosynthesis is a key process in the metabolism of all living organisms. Aminoacyl-tRNA synthetases (aaRSs) play a critical role in protein biosynthesis, since they are responsible for accurate charging of a given set of tRNAs with their cognate amino acids (*25*). Accumulating evidence has indicated that aaRS expression is under the control of regulatory loops in translational feedback regulation in *Escherichia coli* and *S. cerevisiae* (*25, 26*). Likewise, in this work, the RF1 expression was downregulated in the nitrogen-limited sample. In eukaryotes, RF1 (a protein translation release factor) interacted by GTP-bound RF3 in a complex form mediates translation termination (*27*). In *S. cerevisiae*, RF1 levels have been shown to directly correlate with termination efficiency of protein biosynthesis (*28*). Under the downregulation of RF1 expression,

Table 1. Identified Protein Spots of 2-DE Gel Analyses of Cellular Proteins of *M. pilosus* BCRC 31527 Cultivated in the Control Medium and the C/N Ratio 60 Nitrogen-Limited Medium

spot no.	protein identified (M_r/pI)[a]	source	sequence coverage (%)	accession no.[b]	MOWSE score	fold change[c]	type of analysis[d]	database	peptide sequence
S1	glutamyl-tRNA amidotransferase subunit A (GluRS) (52 kDa/4.9)	*Pectobacterium atrosepticum*	20	GATA_STRPN	33	−2	PMF	SwissProt	QPAAFNGIVGLK PTYGTVSRFGLIAFGSSLDQ IGPFAPTVK
S2	cysteinyl-tRNA synthetase (CysRS) (54 kDa/5.4)	*Bacillus licheniformis*	30	SYC_BACLD	51	−2.3	PMF	SwissProt	ADCHPRVTENMDEIIDFIQTLIDK
S3	cysteine synthase (CSase) (32 kDa/5.5)	*Pseudomonas putida* KT2440	38	gil26988386	76	−2.5	PMF	NCBI	LAREEGIFCGVSSGGAVAAMLR
S4	tryptophan synthase α chain (trpA) (29 kDa/6.3)	*Aquifex aeolicus*	29	TRPA_AQUAE	59	−1.9	PMF	SwissProt	IKLICEAADEMTYFVSVTGTTGAR
S5	arginyl-tRNA synthetase (ArgRS) (64 kDa/5.7)	*Neorickettsia sennetsu*	22	SYR_NEOSM	63	−2.8	PMF	SwissProt	LERGFNHMIVGLGADHAGYVK
S6	valyl-tRNA synthetase (ValRS) (103 kDa/7.0)	*Mycoplasma mycoides* subsp. *mycoides* SC	19	SYV_MYCMS	57	−1.5	PMF	SwissProt	MSKSLGNGIDPMDVINNNGCDSLR
S7	D-amino acid dehydrogenase 2 small subunit (dadA) (47 kDa/8.2)	*Pseudomonas putida* KT2440	17	DADA2_PSEPK	34	−2.2	PMF	SwissProt	NLFLNTGHGTLGWTMACGSGR
S8	1-aminocyclopropane-1-carboxylate deaminase (ACCD) (37 kDa/5.6)	*Williopsis saturnus*	31	1A1D_WILSA	49	−1.5	PMF	SwissProt	IVVCCVTGSTTAGILAGMAQYGR
S9	*S*-adenosylmethionine synthetase (MAT) (44 kDa/5.1)	*Methanosarcina mazei*	28	METK_METMA	44	−2.9	PMF	SwissProt	FGGGEVLQPIYMLLVGRATK
S10	*S*-adenosyl methyltransferase mraW (MTase) (35 kDa/8.9)	*Helicobacter pylori* J9	22	MRAW_HELPJ	26	−2.4	PMF	SwissProt	CACSNNHALGAILTKKPITPSPEEIK
S11	ornithine carbamoyltransferase (OCT) (35 kDa/6.3)	*Pyrococcus horikoshii*	29	OTC_PYRHO	33	−2.1	PMF	SwissProt	VSFEVAMAHLGGHALYLNAQDLQLRR
S12	histone deacetylase 1 (HDA) (52 kDa/5.5)	*Caenorhabditis elegans*	25	HDA1_CAEEL	53	2.8	PMF	SwissProt	VMERFDPCAVVLQCGADSLNGDR
S13	DNA-directed RNA polymerase β chain (RNAPβ) (151 kDa/5.5)	*Neorickettsia sennetsu*	17	RPOB_EHRSE	64	1.5	PMF	SwissProt	MAKVIVENMATADFDTVMPCEMINSK
S14	glutamate−cysteine ligase related (GCL) (87 kDa/5.1)	*Enterococcus faecium* DO	22	gil68195404	65	−2.9	PMF	NCBI	AYGIIEANFNPAMHMHVYPFAGKGR
S15	superoxide dismutase (SOD) (22 kDa/7.9)	*Monascus aurantiacus*	23	gil77417963	242	−5.1	LC-MS	NCBI	VTDLPAIVALEPAIK
S16	peroxidase (Px) (25 kDa/5.3)	*Methanosaeta thermophila* PT	34	gil88951648	55	−2.5	PMF	NCBI	FPIIADTGEVADLLGMIHPGK
S17	peptide chain release factor 1 (RF1) (41 kDa/5.0)	*Acinetobacter* sp.	32	RF1_ACIAD	64	−2.7	PMF	SwissProt	YRQAEEDIETAESMLSDPDFK
S18	ATP synthase γ chain (ATPase γ) (33 kDa/9.1)	*Neisseria meningitidis* serogroup B	40	ATPG_NEIMB	54	−2.9	PMF	SwissProt	YLESVVYQALSDNMASEQAARMVAMK
S19	adenylate kinase (AK) (24 kDa/5.1)	*Bacillus clausii*	33	KAD_BACSK	50	−2.1	PMF	SwissProt	IVNDYGIPHISTGDMFRAAMK
S20	UDP-glucose 4-epimerase (GlcE) (35 kDa/7.7)	*Candidatus kuenenia stuttgartiensis*	28	gil91204592	64	1.8	PMF	NCBI	KSVEMPAYDANINILGSLNLCQLSMK
S21	enolase (EN) (48 kDa/5.4)	*Tuber borchii*	10	gil37147852	193	3.2	LC-MS	NCBI	TSDFQIVGDDLTVTNPIR
S22	phosphoenolpyruvate carboxylase (PEPC) (98 kDa/5.4)	*Photobacterium profundum*	19	CAPP_PHOPR	47	1.4	PMF	SwissProt	WGFAVVENSLWHAVPEFLRQFDEK

[a] Theoretical molecular mass (M_r) and theoretical pI of the matched protein in the database. [b] SwissProt or NCBI accession number. [c] Fold change of the significantly altered expression in each protein spot is to compare each spot mean value (from triplicate experiments) with the corresponding mean value of the control and test the expression change using Student's *t*-test. *P* values <0.05 were considered statistically significant. [d] Proteins identified by using MALDI-TOF/TOF-MS through PMF or LC-MS.

the codownregulated expression of the four aaRSs (GluRS, ArgRS, CysRS, and ValRS) in the nitrogen-limited sample may be a reflection of amino acid starvation through a translational feedback regulation in protein biosynthesis, resulting in a decrease in protein translation. In addition, according to that the cellular biomass growth between the nitrogen-limited treatments and the control group had a similar tendency during cultivation, it appeared that the protein biosynthesis in translation in the nitrogen-limited sample was mainly supplied for the demand of the cellular biomass growth.

Another interesting observation is the codownregulation of the three antioxidant-related enzymes (GCL, SOD, and Px), which are involved in the subsequent steps in reactive oxygen species (ROS) metabolism (*29*). In aerobic respiration of filamentous fungus, oxidative phosphorylation of the electron transport chain is the major source of ROS production (including superoxide anion, hydroxyl radical, and hydrogen peroxide), which influences the redox status in cells (*29, 30*). Glutathione acts as a redox buffer and protects cells from damage by reducing the amount of ROS (*31*). Altered glutathione homeostasis, particularly a decrease of glutathione, poses a consequence for ROS production in cells (*31, 32*). GCL is involved in synthesis of glutathione (*31*). The coordinated downregulated expression of GCL and CSase (a cysteine synthase) obviously may result in a decrease of the glutathione pool in cells. In addition, SOD and Px both are responsible for ROS scavenging (*29, 32*). Downregulated expression of these three enzymes may lead to a change of the redox status in the nitrogen-limited cultured cells, due to an increase of the ROS level in the cells. Here, we indicated a link between the nitrogen-limited cultivation of *Monascus* at C/N ratio 60 and the increase of ROS levels in cells via the modulation by protein biosynthesis.

Furthermore, two energy-related enzymes, ATPase γ and AK, revealed downregulation in the nitrogen-limited sample. ATP synthase is known to use a transmembrane electrochemical proton gradient to drive the synthesis of ATP (*33*). AK provides the ADP required for the substrate chain and oxidative phosphorylation and, based on the reversibility of the formation reaction, serves to maintain the "energy charge equilibrium" in cells (*34, 35*). Considering that AK serves essential housekeeping functions in energy metabolism (*34*), it is reasonable that downregulation of AK and ATPase γ is coupled. Increasing evidence has demonstrated ATPases to be sensitive to the redox status in cells *in vitro* (*36, 37*). For example, in *S. cerevisiae*, the activity of vacuolar ATPase, as a thiol enzyme, is modulated by the redox status *in vivo* (*36*). In *Candida* and *Saccharomyces*, ATPases respond to different substrates in nonidentical fashions (*37*). ATPase activity transients reflected morphogenic signals (*33*). The observed underexpression of ATPase γ and AK together therefore appeared to be a reflection of enhanced oxidative stress in the nitrogen-limited cultured cells, implying that the *Monascus* ATPase underexpression repressed ATP generation for providing cellular energy.

Even more interestingly, in contrast to the decreased expression of the proteins previously stated, increased expression was observed for EN, PEPC, GlcE, and two transcriptional regulation enzymes, RNAPβ and HDA, in the nitrogen-limited sample. EN catalyzes the reversible dehydration of D-2-phosphoglycerate (PGA) to phosphoenolpyruvate (PEP) as a key step in both glycolysis and gluconeogenesis (*38*). Accumulating evidence has indicated that EN is a multifunctional protein that plays a crucial role in transcriptional regulation of glycolytic flux (*38, 39*). For example, in *Kluyveromyces lactis*, this enzyme is involved in regulation of glycolytic flux via induction of Rag1 glucose permease expression (*40*). As stated above, ATP generation in cells was suggested to be repressed in the nitrogen-limited cells due to the downregulation of ATPase γ. Moreover, several studies indicated that ATP acts as a potential allosteric effector involved in the regulation of glycolytic and respiratory flux (*38, 39, 41*). In *S. cerevisiae*, the role of ATP in the regulation of metabolic shift was correlated with mitochondrial transcription and RNAP expression (*42, 43*). RNAPs are responsible for stable RNA synthesis in transcription (*44*), and HDA contributes to the regulation of transcription (*45*). In *E. coli*, the nitrogen regulation system is a complex regulatory cascade that senses the quality of the available nitrogen supply and ultimately results in the activation of a transcriptional activator (NtrC), when the nitrogen source is growth rate limiting (*46*). Many of the *E. coli* genes in the nitrogen regulon are directly regulated by the NtrC-mediated activation of RNAP (*46*). Under the downregulated ATPase expression, the observed coordinated upregulation of EN with RNAPβ and HDA together may indicate an increase of glycolytic flux, acting through ATP level depletion in transcriptional regulation, in an attempt to maintain metabolic energy homeostasis in the nitrogen-limited cultured filamentous cells.

The allosteric enzyme PEPC branches from glycolysis through a carboxylation reaction to replenish intermediate pools (such as acetyl-CoA) for the TCA cycle (*47, 48*). Acetyl-CoA is a powerful allosteric activator of PEPC in many species of organisms (*47, 48*). In obligate aerobes, such as *Monascus*, the switch of metabolic flux from glycolysis into the TCA cycle through oxidative phosphorylation for ATP generation proceeds with a high yield of ATP (*38*). In aerobic *Monascus* cultivation under the nitrogen limitation at C/N ratio 60, the polyketide red pigment production was inhibited (**Figure 1B**). However, polyketide biosynthesis begins with using acetyl-CoA as a building block. In this respect, the detected upregulation of PEPC with an opposite suppression in red pigment production suggested that the metabolic flux shift of acetyl-CoA was to the TCA cycle for more ATP generation through oxidative phosphorylation, not switching to the biosynthetic polyketide pathway for red pigment formation. In addition, GlcE, a highly conserved enzyme, catalyzes the interconversion of UDP-galactose and UDP-glucose, playing the pivotal role in cellular assembly of complex polysaccharides and other glycosylated macromolecules (*49*). Compared to the control, the nitrogen-limited treatment did not result in significant suppression of cell growth (**Figure 1A**). Considering the biological significance of GlcE, its upregulation in the nitrogen-limited cells may indicate that the treated cultured cells attempted to maintain the cell growth under nitrogen limitation-induced ATP level starvation status.

In the literature, in the *S. cerevisiae* response to nitrogen limitation, the cells trigger a complicated metabolic rearrangement via several signal pathways involved in carbon and nitrogen metabolism to adapt to changed conditions for cell survival (*50*). Taken together, in this work, compared to the control (C/N ratio 20), the nitrogen-limited cultivation (C/N ratio 60) of *M. pilosus* BCRC 31527 did not significantly affect the cellular biomass growth but suppressed red pigment production during the stationary phase. Moreover, our proteomic comparison between the control and treated filamentous cells revealed that the nitrogen limitation induced the altered expression of proteins involved in amino acid biosynthesis, protein translation, antioxidant-related enzymes, glycolysis, and transcriptional regulation. In the nitrogen-limited sample, the observed downregulation of antioxidant-related enzymes, caused by the sup-

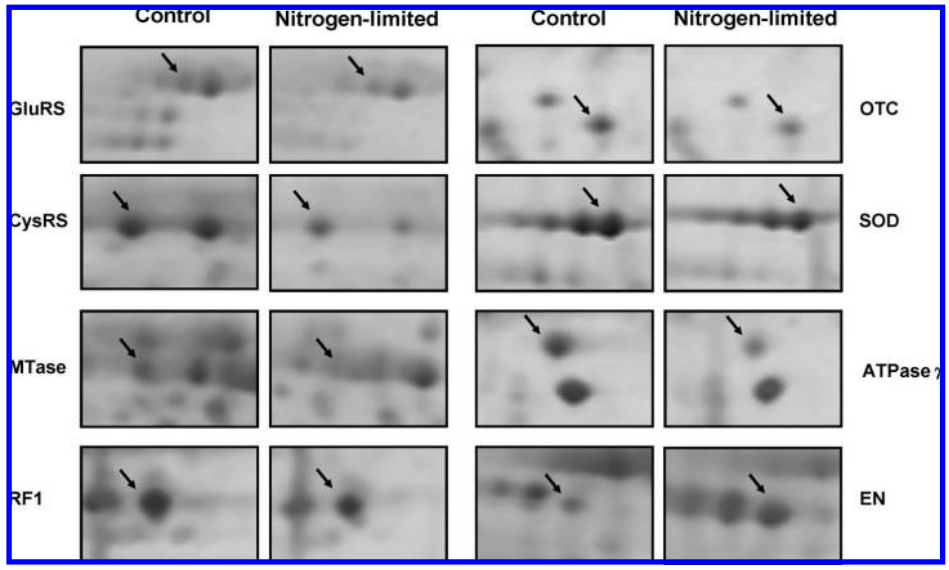

Figure 3. Enlarged view of the detailed alteration patterns of the eight representative protein spots from 2-DE gel maps in **Figure 2** (differentially expressed between the C/N ratio 20 control and the C/N ratio 60 nitrogen-limited samples).

pression of protein translation under the nitrogen limitation, suggested that an increase of ROS level in the nitrogen-limited cultured cells was induced. Following a cellular redox status modulation of the ATPase expression, subsequently, it led to the energy-generating enzyme ATPase underexpression, which, in turn, resulted in lower ATP generation for the cellular energy demand. In this respect, therefore, it is reasonable that the nitrogen limitation at C/N ratio 60, coupled with the suppression in red pigment production, induced a switch of metabolic flux from glycolysis to the TCA cycle for oxidative phosphorylation in an effort to maintain cellular energy homeostasis, instead of shifting to the polyketide biosynthesis pathway for red pigment production. As stated above, using acetyl-CoA as the building block, the biosynthesis of many *Monascus* polyketide secondary metabolites, including pigments and citrinin, involves the formation of tetraketide as the precursor intermediate to form polyketides. The results obtained showed that, compared to the control, the nitrogen limitation in nitrogen metabolism at C/N ratio 60 in *M. pilosus* BCRC 31527 appeared to affect the flux shift of carbon metabolism, which was driven toward energy generation. It seemed that the triggering of polyketide biosynthesis in *Monascus* was linked to nitrogen metabolism. The impact of C/N ratios and role of nitrogen metabolism in the onset of the biosynthesis of polyketides from carbon anabolism should be further realized through their involvement in setting of the direction of carbon fluxes. In this work, understanding the biochemical events involved in nitrogen limitation and the influence of metabolic flux shift on *Monascus* cultivation will have practical applications for the improvement of the industrial production of secondary metabolites of the fungus.

ABBREVIATIONS USED

aaRSs, aminoacyl-tRNA synthetases; ACC, aminocyclopropane-1-carboxylate; ACCD, 1-aminocyclopropane-1-carboxylate deaminase; ACN, acetonitrile; AdoMet, *S*-adenosylmethionine; AK, adenylate kinase; ArgRS, arginyl-tRNA synthetase; ATPase γ, ATP synthase F1 γ subunit; CHAPS, 3-[(3-cholamidopropyl)dimethylammonio]-1-propanesulfonate; CHCA, α-cyano-4-hydroxycinnamic acid; CSase, cysteine synthase; CysRS, cysteinyl-tRNA synthetase; dadA, D-amino acid dehydrogenase 2; DTT, dithiothreitol; EN, enolase; GCL, glutamate−cysteine ligase; GlcE, UDP-glucose 4-epimerase; GluRS, glutaminyl-tRNA synthase; HDA, histone deacetylase 1; IAA, iodoacetamide; IPG, immobilized pH gradients; MAT, *S*-adenosylmethionine synthetase; MTase, *S*-adenosyl methyltransferase mraW; OTC, ornithine carbamoyltransferase; PEPC, phosphoenolpyruvate carboxylase; Px, peroxidase; RF1, peptide chain release factor 1; RNAPβ, DNA-directed RNA polymerase β chain; ROS, reactive oxygen species; SDS, sodium dodecyl sulfate; SOD, superoxide dismutase; TCA, tricarboxylic acid; trpA, tryptophan synthase α chain; ValRS, valyl-tRNA synthetase.

ACKNOWLEDGMENT

We gratefully thank Cheng-Chung Liao, Ph.D., from the Institute of Biochemistry, National Yang Ming University, for technical assistance with MALDI-TOF/TOF-MS.

LITERATURE CITED

(1) Hajjaj, H.; Blanc, P. J.; Groussac, E.; Goma, G.; Uribelarrea, J. L.; Loubiere, P. Improvement of red pigment/citrinin production ratio as a function of environmental conditions by *Monascus ruber*. *Biotechnol. Bioeng.* **1999**, *64*, 497–501.

(2) Endo, A.; Hasumi, K. Biochemical aspect of HMG CoA reductase inhibitors. *Adv. Enzyme Regul.* **1989**, *28*, 53–64.

(3) Hajjaj, H.; Klaebe, A.; Loret, M. O.; Goma, G.; Blanc, P. J.; Francois, J. Biosynthetic pathway of citrinin in the filamentous fungus *Monascus ruber* as revealed by ^{13}C nuclear magnetic resonance. *Appl. Environ. Microbiol.* **1999**, *65*, 311–314.

(4) Shimizu, T.; Kinoshita, H.; Ishihara, S.; Sakai, K.; Nagai, S.; Nihira, T. Polyketide synthase gene responsible for citrinin biosynthesis in *Monascus purpureus*. *Appl. Environ. Microbiol.* **2005**, *71*, 3453–3457.

(5) Marzluf, G. A. Genetic regulation of nitrogen metabolism in the fungi. *Microbiol. Mol. Biol. Rev.* **1997**, *61*, 17–32.

(6) Wu, J.; Zhang, N.; Hayes, A.; Panoutsopoulou, K.; Oliver, S. G. Global analysis of nutrient control of gene expression in *Saccharomyces cerevisiae* during growth and starvation. *Proc. Natl. Acad. Sci. U.S.A.* **2004**, *101*, 3148–3153.

(7) Wang, J. J.; Lee, C. L.; Pan, T. M. Modified mutation method for screening low citrinin-producing strains of *Monascus purpureus* on rice culture. *J. Agric. Food Chem.* **2004**, *52*, 6977–6982.

(8) Thomsson, E.; Gustafsson, L.; Larsson, C. Starvation response of *Saccharomyces cerevisiae* grown in anaerobic nitrogen- or carbon-limited chemostat cultures. *Appl. Environ. Microbiol.* **2005**, *71*, 3007–3013.

(9) Lin, W. Y.; Ting, Y. C.; Pan, T. M. Proteomic response to intracellular proteins of *Monascus pilosus* grown under phosphate-limited complex medium with different growth rates and pigment production. *J. Agric. Food Chem.* **2007**, *55*, 467–474.
(10) Lin, W. Y.; Chang, J. Y.; Tsai, P. C.; Pan, T. M. Metabolic protein patterns and monascorubrin production revealed through proteomic approach for *Monascus pilosus* treated with cycloheximide. *J. Agric. Food Chem.* **2007**, *55*, 5559–5568.
(11) Teng, S. S.; Feldheim, W. Anka and anka pigment production. *J. Ind. Microbiol. Biotechnol.* **2001**, *26*, 280–282.
(12) Hajjaj, H.; Klaebe, A.; Loret, M. O.; Tzedakis, T.; Goma, G.; Blanc, P. J. Production and identification of N-glucosylrubropunctamine and N-glucosylmonascorubramine from *Monascus ruber* and occurrence of electron donor-acceptor complexes in these red pigments. *Appl. Environ. Microbiol.* **1997**, *63*, 2671–2678.
(13) Grinyer, J.; McKay, M.; Herbert, B.; Nevalainen, H. Fungal proteomics: mapping the mitochondrial proteins of a *Trichoderma harzianum* strain applied for biological control. *Curr. Genet.* **2004**, *45*, 170–175.
(14) Lin, W. Y.; Song, C. Y.; Pan, T. M. Proteomic analysis of Caco-2 cells treated with monacolin K. *J. Agric. Food Chem.* **2006**, *54*, 6192–6200.
(15) Cordwell, S. J.; Wilkins, M. R.; Cerpa-Poljak, A.; Gooley, A. A.; Duncan, M.; Williams, K. L.; Humphery-Smith, I. Cross-species identification of proteins separated by two-dimensional gel electrophoresis using matrix-assisted laser desorption ionisation/time-of-flight mass spectrometry and amino acid composition. *Electrophoresis* **1995**, *16*, 438–443.
(16) Faulhammer, F.; Konrad, G.; Brankatschk, B.; Tahirovic, S.; Knodler, A.; Mayinger, P. Cell growth-dependent coordination of lipid signaling and glycosylation is mediated by interactions between Sac1p and Dpm1p. *J. Cell Biol.* **2005**, *168*, 185–191.
(17) Donofrio, N. M.; Oh, Y.; Lundy, R.; Pan, H.; Brown, D. E.; Jeong, J. S.; Coughlan, S.; Mitchell, T. K.; Dean, R. A. Global gene expression during nitrogen starvation in the rice blast fungus *Magnaporthe grisea*. *Fungal Genet. Biol.* **2006**, *43*, 605–617.
(18) Marzluf, G. A. Molecular genetics of sulfur assimilation in filamentous fungi and yeast. *Annu. Rev. Microbiol.* **1997**, *51*, 73–96.
(19) Prudova, A.; Bauman, Z.; Braun, A.; Vitvitsky, V.; Lu, S. C.; Banerjee, R. S-adenosylmethionine stabilizes cystathionine beta-synthase and modulates redox capacity. *Proc. Natl. Acad. Sci. U.S.A.* **2006**, *103*, 6489–6494.
(20) Kalhor, H. R.; Penjwini, M.; Clarke, S. A novel methyltransferase required for the formation of the hypermodified nucleoside wybutosine in eucaryotic tRNA. *Biochem. Biophys. Res. Commun.* **2005**, *334*, 433–440.
(21) Jacobson, E. S.; Metzenberg, R. L. Control of arylsulfatase in a serine auxotroph of Neurospora. *J. Bacteriol.* **1977**, *130*, 1397–1398.
(22) Zhao, Z.; Chen, H.; Li, K.; Du, W.; He, S.; Liu, H. W. Reaction of 1-amino-2-methylenecyclopropane-1-carboxylate with 1-aminocyclopropane-1-carboxylate deaminase: analysis and mechanistic implications. *Biochemistry* **2003**, *42*, 2089–2103.
(23) Crabeel, M.; Lavalle, R.; Glansdorff, N. Arginine-specific repression in *Saccharomyces cerevisiae*: kinetic data on ARG1 and ARG3 mRNA transcription and stability support a transcriptional control mechanism. *Mol. Cell. Biol.* **1990**, *10*, 1226–1233.
(24) Tang, X. F.; Ezaki, S.; Atomi, H.; Imanaka, T. Biochemical analysis of a thermostable tryptophan synthase from a hyperthermophilic archaeon. *Eur. J. Biochem.* **2000**, *267*, 6369–6377.
(25) Burke, D. J.; Church, D. Protein synthesis requirements for nuclear division, cytokinesis, and cell separation in *Saccharomyces cerevisiae*. *Mol. Cell. Biol.* **1991**, *11*, 3691–3698.
(26) Grundy, F. J.; Henkin, T. M. Conservation of a transcription antitermination mechanism in aminoacyl-tRNA synthetase and amino acid biosynthesis genes in gram-positive bacteria. *J. Mol. Biol.* **1994**, *235*, 798–804.
(27) Polevoda, B.; Span, L.; Sherman, F. The yeast translation release factors Mrf1p and Sup45p (eRF1) are methylated, respectively, by the methyltransferases Mtq1p and Mtq2p. *J. Biol. Chem.* **2006**, *281*, 2562–2571.
(28) Stansfield, I.; Eurwilaichitr, L.; Akhmaloka; Tuite, M. F. Depletion in the levels of the release factor eRF1 causes a reduction in the efficiency of translation termination in yeast. *Mol. Microbiol.* **1996**, *20*, 1135–1143.
(29) Cyrne, L.; Martins, L.; Fernandes, L.; Marinho, H. S. Regulation of antioxidant enzymes gene expression in the yeast *Saccharomyces cerevisiae* during stationary phase. *Free Radical Biol. Med.* **2003**, *34*, 385–393.
(30) Lushchak, V.; Semchyshyn, H.; Mandryk, S.; Lushchak, O. Possible role of superoxide dismutases in the yeast *Saccharomyces cerevisiae* under respiratory conditions. *Arch. Biochem. Biophys.* **2005**, *441*, 35–40.
(31) Kim, S. J.; Park, E. H.; Lim, C. J. Stress-dependent regulation of the gene encoding gamma-glutamylcysteine synthetase from the fission yeast. *Mol. Biol. Rep.* **2004**, *31*, 23–30.
(32) Campos, E. G.; Jesuino, R. S.; Dantas Ada, S.; Brigido Mde, M.; Felipe, M. S. Oxidative stress response in *Paracoccidioides brasiliensis*. *Genet. Mol. Res.* **2005**, *4*, 409–429.
(33) Velours, J.; Arselin, G. The *Saccharomyces cerevisiae* ATP synthase. *J. Bioenerg. Biomembr.* **2000**, *32*, 383–390.
(34) Schricker, R.; Angermayr, M.; Strobel, G.; Klinke, S.; Korber, D.; Bandlow, W. Redundant mitochondrial targeting signals in yeast adenylate kinase. *J. Biol. Chem.* **2002**, *277*, 28757–28764.
(35) Schricker, R.; Magdolen, V.; Strobel, G.; Bogengruber, E.; Breitenbach, M.; Bandlow, W. Strain-dependent occurrence of functional GTP:AMP phosphotransferase (AK3) in *Saccharomyces cerevisiae*. *J. Biol. Chem.* **1995**, *270*, 31103–31110.
(36) Oluwatosin, Y. E.; Kane, P. M. Mutations in the CYS4 gene provide evidence for regulation of the yeast vacuolar H^+-ATPase by oxidation and reduction in vivo. *J. Biol. Chem.* **1997**, *272*, 28149–28157.
(37) Fernandes, A. R.; Sa-Correia, I. Transcription patterns of PMA1 and PMA2 genes and activity of plasma membrane H^+-ATPase in *Saccharomyces cerevisiae* during diauxic growth and stationary phase. *Yeast* **2003**, *20*, 207–219.
(38) Larsson, C.; Pahlman, I. L.; Gustafsson, L. The importance of ATP as a regulator of glycolytic flux in *Saccharomyces cerevisiae*. *Yeast* **2000**, *16*, 797–809.
(39) Larsson, C.; Nilsson, A.; Blomberg, A.; Gustafsson, L. Glycolytic flux is conditionally correlated with ATP concentration in *Saccharomyces cerevisiae*: a chemostat study under carbon- or nitrogen-limiting conditions. *J. Bacteriol.* **1997**, *179*, 7243–7250.
(40) Lemaire, M.; Wesolowski-Louvel, M. Enolase and glycolytic flux play a role in the regulation of the glucose permease gene RAG1 of *Kluyveromyces lactis*. *Genetics* **2004**, *168*, 723–731.
(41) Beauvoit, B.; Bunoust, O.; Guerin, B.; Rigoulet, M. ATP-regulation of cytochrome oxidase in yeast mitochondria: role of subunit VIa. *Eur. J. Biochem.* **1999**, *263*, 118–127.
(42) Westergaard, S. L.; Oliveira, A. P.; Bro, C.; Olsson, L.; Nielsen, J. A systems biology approach to study glucose repression in the yeast *Saccharomyces cerevisiae*. *Biotechnol. Bioeng.* **2007**, *96*, 134–145.
(43) Amiott, E. A.; Jaehning, J. A. Mitochondrial transcription is regulated via an ATP "sensing" mechanism that couples RNA abundance to respiration. *Mol. Cell* **2006**, *22*, 329–338.
(44) Clarke, E. M.; Peterson, C. L.; Brainard, A. V.; Riggs, D. L. Regulation of the RNA polymerase I and III transcription systems in response to growth conditions. *J. Biol. Chem.* **1996**, *271*, 22189–22195.
(45) Kouzarides, T. Histone acetylases and deacetylases in cell proliferation. *Curr. Opin. Genet. Dev.* **1999**, *9*, 40–48.
(46) Muse, W. B.; Rosario, C. J.; Bender, R. A. Nitrogen regulation of the codBA (cytosine deaminase) operon from *Escherichia coli* by the nitrogen assimilation control protein, NAC. *J. Bacteriol.* **2003**, *185*, 2920–2926.
(47) Chen, L. M.; Li, K. Z.; Miwa, T.; Izui, K. Overexpression of a cyanobacterial phosphoenolpyruvate carboxylase with diminished sensitivity to feedback inhibition in *Arabidopsis* changes amino acid metabolism. *Planta* **2004**, *219*, 440–449.

(48) Lin, H.; Vadali, R. V.; Bennett, G. N.; San, K. Y. Increasing the acetyl-CoA pool in the presence of overexpressed phosphoenolpyruvate carboxylase or pyruvate carboxylase enhances succinate production in *Escherichia coli*. *Biotechnol. Prog.* **2004**, *20*, 1599–1604.

(49) Ross, K. L.; Davis, C. N.; Fridovich-Keil, J. L. Differential roles of the Leloir pathway enzymes and metabolites in defining galactose sensitivity in yeast. *Mol. Genet. Metab.* **2004**, *83*, 103–116.

(50) Kolkman, A.; Daran-Lapujade, P.; Fullaondo, A.; Olsthoorn, M. M.; Pronk, J. T.; Slijper, M.; Heck, A. J. Proteome analysis of yeast response to various nutrient limitations. *Mol. Syst. Biol.* **2006**, *2*, 2006–0026.

Received for review August 12, 2007. Revised manuscript received October 31, 2007. Accepted November 15, 2007.

JF072420E